How much fuel and time can be saved in a *perfect* flight trajectory?

Continuous cruise climbs *vs.* conventional operations

Ramon Dalmau Xavier Prats
Technical University of Catalonia
Castelldefels, Barcelona (Spain)
Email: ramon.dalmau@estudiant.upc.edu, xavier.prats@upc.edu

***Abstract*—Continuous climb, cruise and decent operations (referred as continuous operations) may contribute to significantly reduce fuel and emissions. Nevertheless, it is obvious that the introduction of such procedures at large scale is not possible with the current air traffic management concept of operations, since flying at constant altitudes is one of the key aspects to strategically separate flows of aircraft. This paper tries to quantify what would be the potential savings of flying such optimised vertical profiles. A multiphase optimal control problem is formulated and solved by means of numerical optimisation. Optimal conventional trajectories (subject to realistic air traffic management practices and constraints) are compared with optimal continuous (and ideal) operations, only subject to aircraft performance constraints. Results show that the continuous cruise phase can lead to fuel savings between 1% and 2% of the total trip fuel for an Airbus A320. Interestingly, continuous operations show also a reduction of trip times between 1% and 5% of the total trip time, depending on the trip distance between origin and destination airports.**

I. Introduction

In air transportation, gaseous emissions, noise and local air quality remain major issues. At present, reducing fuel consumption (and therefore emissions) is perhaps one of the main concerns of the different aviation stakeholders. According to [1], in 2008 fuel was the largest single cost item for the global airline industry, representing more than the 30% of the total operating cost. An optimal flight vertical profile in terms of minimising fuel consumption is not composed by level segments at constant (cruise) altitudes. In fact, the optimal profile consists of a continuous climb, with a climb rate that reduces progressively as long as the aircraft approaches the altitude where drag is a global minimum, followed by a continuous descent with the engines at idle [2]–[7].

As it is well known, however, in the current concept of operations (ConOps) aircraft are asked to fly at constant cruise altitudes. In this way, strategic separation is provided and the air traffic control (ATC) tasks to maintain safe separation among all aircraft are much more simplified. Furthermore, climbs and descents are usually interrupted by segments of level flight at constant altitude in order to maintain separation of crossing flows in a terminal manoeuvring area (TMA). Separation management may also deviate trajectories from their optimum in the lateral (horizontal) domain (i.e. direct routings), since in busy TMA path stretching and radar vectoring are common ATC practices.

The design and assessment of optimal vertical flight profiles for commercial aircraft has been studied in the last decades mainly focusing in TMA operations – i.e. with continuous descent operations (CDO) and continuous climb operations (CCO). See for instance [8]–[10] and the references therein. Optimal cruise procedures, according to the current (constrained) ConOps have been assessed, as optimal control problems, in [11] or [12] for example. In [4], a discrete search algorithm, with a rather simplistic aircraft performance model, was used to optimise trajectories finding also progressive cruise climbs as optimal vertical profiles. A very complete and promising aircraft trajectory optimisation framework is presented in [3], showing also a comparison between a conventional vertical flight profile and an optimised profile with continuous climb, cruise and descent operations.

The conclusions arising from these works show the advantages of such continuous operations. The actual quantitative benefits, however, in terms of fuel savings and accurate determination of the optimal vertical trajectories, are hard to assess mainly due to approximations in aircraft and engine performance models. Refs. [2] and [13], for instance, show the importance to take into account air compressibility effects into aerodynamic drag equations, which are typically ignored in several performance models – such as the widely used Eurocontrol's Base of aircraft data (BADA, version 3.6 or lower). Accurate engine models are also very important to take into account, since actual engine performance and limitations have a great impact on the maximum and optimum flight altitudes and therefore, on the optimal speed profiles and trip time and fuel figures.

The majority of the previous cited works (see for instance [3]–[5]) do not consider some important operational restrictions when optimising current conventional trajectories, such as a minimum rate of climb. Furthermore, Refs. [3], [6], [12] focused on the development of the mathematical framework to derive very valuable optimisation algorithms, but almost none attempted to accurately quantify the benefits of continuous operations considering the flight as a whole.

In this paper, the entire aircraft trajectory will be subject of optimisation, from the take-off to landing and two specific situations will be analysed: current conventional operations, considering realistic and accurate current ATC constraints and

limitations on the flight; and continuous operations comprising an uninterrupted and continuous climb, followed by a continuous descent. In both cases accurate aircraft performance data, derived from Airbus Performance Engineering Programs (PEP)[1], have been used to model drag, engine thrust and fuel flow. Thus, the main contribution of this paper is to try to quantify the benefits of such *perfect* trajectory or ideal operations for several trip distances and aircraft landing masses, aiming at motivating future research efforts and technologies to make them possible.

II. Background

The optimisation of an aircraft trajectory, as a 4 dimensional continuum, is a multi-phase constrained optimal control problem. These kinds of problems are not easy to solve, especially when nonlinear functions appear in the definition of the optimisation objective and/or the constraints [14].

Generally speaking, optimal control problems for *real world* applications do not have analytic solutions and typically, numerical methods are used to solve them. In the last decade, with the availability of more powerful computers, numeric approaches are enabling to solve realistic problems in short computational times. There are several ways to address these type of problems and in this study the direct collocation method described in [15] has been used. Such direct methods transform the original continuous (and thus infinite) optimal control problem into a (discrete and finite) nonlinear programming (NLP) optimisation problem. The advantage of these methods is the possibility of solving very complex problems with a minimum effort of mathematical analysis. In fact, only the physical equations need to be coded and the necessary conditions do not have to be derived. Therefore, the direct collocation methods can be used to solve a wide amount of practical problems, such as trajectory optimisation problems for commercial aircraft typical missions [12].

A. Optimal control problem formulation

Let us divide the trajectory optimisation problem into N phases. For each phase $i \in \{1, N\}$, defined over the time period $[t_0^{(i)}, t_f^{(i)}]$, a state vector $\boldsymbol{x}^{(i)}(t)$, a control vector $\boldsymbol{u}^{(i)}(t)$ and parameter vector[2] $\boldsymbol{p}^{(i)}$ are defined. The goal of an optimal control problem is to find the best control and parameter vector functions for each phase that minimise a given cost functional J, defined over the whole time period $[t_0^{(1)}, t_f^{(N)}]$:

$$J\left(\boldsymbol{x}^{(1)}(t), \boldsymbol{u}^{(1)}(t), \boldsymbol{p}^{(1)}, \boldsymbol{x}^{(2)}(t), \boldsymbol{u}^{(2)}(t), \boldsymbol{p}^{(2)}, \ldots, \boldsymbol{x}^{(N)}(t), \boldsymbol{u}^{(N)}(t), \boldsymbol{p}^{(N)}\right). \tag{1}$$

Notice that the cost functional may depend on quantities computed in each of the N phases. In order to guarantee a feasible and acceptable trajectory, as a result of this optimisation process, several constraints must be considered. In particular the dynamics of the system (dynamics of the state vector), expressed by non-linear vector functions $f^{(i)}$ as:

$$\frac{\mathrm{d}\boldsymbol{x}^{(i)}}{\mathrm{d}t} = \dot{\boldsymbol{x}}^{(i)}(t) = f^{(i)}\left(\boldsymbol{x}^{(i)}(t), \boldsymbol{u}^{(i)}(t), \boldsymbol{p}^{(i)}, t\right). \tag{2}$$

In addition, the solution might satisfy some algebraic event constraints $\boldsymbol{e}^{(i)}$ (i.e. initial and final conditions at the different phases), expressed in the general form with vector functions:

$$\begin{aligned}\boldsymbol{e}_L^{(i)} \leqslant \boldsymbol{e}^{(i)}\Big(&\boldsymbol{x}^{(i)}(t_0^{(i)}), \boldsymbol{x}^{(i)}(t_f^{(i)}), \boldsymbol{u}^{(i)}(t_0^{(i)}),\\ &\boldsymbol{u}^{(i)}(t_f^{(i)}), \boldsymbol{p}^{(i)}\Big) \leqslant \boldsymbol{e}_U^{(i)},\end{aligned} \tag{3}$$

some algebraic path constraints $\boldsymbol{h}^{(i)}$ such as

$$\boldsymbol{h}_L^{(i)} \leqslant \boldsymbol{h}^{(i)}\left(\boldsymbol{x}^{(i)}(t), \boldsymbol{u}^{(i)}(t), \boldsymbol{p}^{(i)}\right) \leqslant \boldsymbol{h}_U^{(i)} \tag{4}$$

and simple bounds on the state, control and time variables (box constraints):

$$\begin{aligned}&\boldsymbol{x}_L^{(i)}(t) \leqslant \boldsymbol{x}^{(i)}(t) \leqslant \boldsymbol{x}_U^{(i)}(t) && t_{0_L}^{(i)} \leqslant t_0^{(i)} \leqslant t_{0_U}^{(i)}\\ &\boldsymbol{u}_L^{(i)}(t) \leqslant \boldsymbol{u}^{(i)}(t) \leqslant \boldsymbol{u}_U^{(i)}(t) && t_{f_L}^{(i)} \leqslant t_f^{(i)} \leqslant t_{f_U}^{(i)}.\\ &\boldsymbol{p}_L^{(i)} \leqslant \boldsymbol{p}^{(i)} \leqslant \boldsymbol{p}_U^{(i)}\end{aligned} \tag{5}$$

For those problems defined over more than one phase, the dynamics of the system, the event, path and box constraints might be different. However, it might be desirable to link some state variables across two consecutive phases, in order to enforce some continuity to those variables. This leads to another set of constraints also known as link constraints $\boldsymbol{\Psi}$:

$$\begin{aligned}\boldsymbol{\Psi}_L \leqslant \boldsymbol{\Psi}\Big(&\boldsymbol{x}^{(1)}(t_0^{(1)}), \boldsymbol{x}^{(1)}(t_f^{(1)}), t_0^{(1)}, t_f^{(1)},\\ &\boldsymbol{x}^{(2)}(t_0^{(2)}), \boldsymbol{x}^{(2)}(t_f^{(2)}), t_0^{(2)}, t_f^{(2)}, \ldots,\\ &\boldsymbol{x}^{(N)}(t_0^{(N)}), \boldsymbol{x}^{(N)}(t_f^{(N)}), t_0^{(N)}, t_f^{(N)}\Big) \leqslant \boldsymbol{\Psi}_U.\end{aligned} \tag{6}$$

In the previous notation, $(\cdot)_L$ and $(\cdot)_U$ are respectively the lower and upper bounds for these constraints. It should be noted that equality constraints can be defined by setting the lower bound equal to the upper bound, i.e. $(\cdot)_L = (\cdot)_U$.

B. NLP transcription and starting point

Collocation methods discretise the time histories of control and state variable at a set of nodal or collocation points, being the system of ordinary differential equations (2) approximated by some continuous function (such as polynomials) over each collocation step. The values of these discretised variables, along with the non-time dependent parameters, become the unknowns of the new finite variable problem, which can be formally as a NLP problem and solved by standard NLP solvers. Several collocation schemes are proposed in the literature, being the trapezoidal collocation method the approach used in this paper. Trapezoidal collocation shows a good trade-off

[1] Airbus PEP software provides high degree of precision in the certified aircraft performance data and uses specific Flight Management System (FMS) algorithms for the computations.

[2] formally defined as a vector of variables that are not time dependent

between accuracy and execution time needed to solve highly constrained NLP problems [14].

NLP solvers are always executed from a starting point with all the variables of the problem (unknowns of the problem) initialised to some value. Typically, the user can specify these starting values and otherwise, the solver will just set all the unknowns to zero or to another random value. Then, from this starting point, the internal algorithm of the NLP solver aims to find a feasible (i.e. that fulfils all the constraints) and optimal (i.e. that minimises/maximises the cost functional) solution.

An appropriate starting point or initial *guess* can dramatically reduce the convergence time of the optimisation, being for some complex problems, a key aspect influencing the solver's success on convergence too, which cannot even converge if the guess solution is not good enough [16]. It should be noted that, since NLP solvers cannot guarantee a global optimum, different initial guesses could lead to different sub-optimal solutions.

III. Aircraft performance model

In this section the aircraft dynamic equations, along with drag and engine performance models, are presented. A nonlinear point-mass representation of the aircraft (where forces are applied at its centre of gravity) is used. The aircraft dynamics are described in the air reference frame assuming flat non-rotating earth and neglecting wind components [17]:

$$\begin{aligned} \frac{\mathrm{d}v}{\mathrm{d}t} &= \dot{v} = \frac{T-D}{m} - g\sin\gamma \\ \frac{\mathrm{d}s}{\mathrm{d}t} &= \dot{s} = v\cos\gamma \\ \frac{\mathrm{d}h}{\mathrm{d}t} &= \dot{h} = v\sin\gamma \\ \frac{\mathrm{d}m}{\mathrm{d}t} &= \dot{m} = -FF \end{aligned} \tag{7}$$

where the state vector $\boldsymbol{x} = [v, s, h, m]$ is formed respectively, by the true airspeed, the along path distance, altitude and the mass of the aircraft; T is the total thrust; D is the aerodynamic drag; g is the gravity acceleration (assumed to be constant); γ is the aerodynamic flight path angle and FF is the fuel flow.

The control vector considered is $\boldsymbol{u} = [\pi, \gamma]$, where π is the throttle setting.

Regarding the atmosphere, the International Standard Atmosphere [18] model is considered, which defines the density ρ, pressure p and temperature τ magnitude as functions of the altitude. The following normalised magnitudes are also used in this paper:

$$\delta = \frac{p}{p_0}; \quad \theta = \frac{\tau}{\tau_0}; \quad \sigma = \frac{\rho}{\rho_0}; \tag{8}$$

where p_0, τ_0 and ρ_0 are, respectively the standard pressure, temperature and density values at sea level.

Operational constraints are usually given in terms of the Mach number $M = v/v_c$ (being v_c the speed of sound) or calibrated airspeed (CAS), which is computed as a function of the true airspeed and atmospheric magnitudes as follows:

$$v_{CAS} = \sqrt{\frac{2p_0}{\mu\rho_0}\left[\left(\delta\left(\left(\frac{\mu v^2}{2R\tau}+1\right)^{\frac{1}{\mu}}-1\right)+1\right)^{\mu}-1\right]} \tag{9}$$

where $\mu = \frac{\gamma_a - 1}{\gamma_a}$ and $v_c = \sqrt{\gamma_a R\tau}$; being γ_a the specific heat ratio of the air and R the perfect gases constant.

All aerodynamic and engine parameters are represented by continuous polynomials, that ensure continuity for the first and second derivatives as it is required for numerical reasons by NLP solvers. These models are described below.

A. Drag model

The aerodynamic drag is modelled as:

$$D = \frac{1}{2}\rho S v^2 C_D \tag{10}$$

where C_D is the drag coefficient and S the wing area.

The drag coefficient is expressed as a function of the lift coefficient C_L and M. This relationship considers air compressibility effects, which cannot be neglected for nominal cruising speeds of typical commercial aircraft (between M.78 and M.82 approximately). In this paper, a polynomial fitting similar to the model proposed in [13] is used, giving a very accurate approximation of the drag coefficient:

$$C_D = C_{D0} + K_i(C_L - C_{L0})^2. \tag{11}$$

Coefficients C_{D0}, K_i and C_{L0} depend on the flaps/slats setting and M. For each aircraft configuration these coefficients are obtained after a fitting function process with aircraft aerodynamic data obtained from PEP's data base:

$$\begin{aligned} C_{D0} &= C_{D0_{min}} + \Delta C_{D0} M \\ K_i &= K_{i_{min}} + \Delta K_{i_1} M + \Delta K_{i_2} M^2 \\ C_{L0} &= C_{L0_{min}} + \Delta C_{L0_1} M + \Delta C_{L0_2} M^2. \end{aligned} \tag{12}$$

B. Engine model

Typically, throttle setting ($\pi \in [0,1]$) directly commands the revolutions of the engine fan ($N1$):

$$\pi = \frac{N1 - N1_{idle}}{N1_{max} - N1_{idle}}. \tag{13}$$

The maximum revolutions of the engine fan $N1_{max}$ and the residual revolutions, when the throttle is zero ($N1_{idle}$) are modelled with a third degree polynomial approximation as:

$$N1_k = \sum_{i=0}^{3}\sum_{j=0}^{3} c_{ij}^k \theta^i M^j \quad k \in \{max, idle\}. \tag{14}$$

Following the same methodology, T and FF are also modelled by a third order polynomial as a function of the reduced revolutions of the engine fan ($N1/\sqrt{\theta}$) and M [19]:

$$T = n_e \delta \sum_{i=0}^{3}\sum_{j=0}^{3} c_{ij}^{T} \left(\frac{N1}{\sqrt{\theta}}\right)^i M^j$$
$$FF = n_e \delta \sqrt{\theta} \sum_{i=0}^{3}\sum_{j=0}^{3} c_{ij}^{FF} \left(\frac{N1}{\sqrt{\theta}}\right)^i M^j \quad (15)$$

being n_e the number of engines of the airplane.

IV. Trajectory optimisation

The optimisation process presented in this paper is a constrained non-lineal optimal control problem, as defined in section II. This study aims at computing minimum trip fuel trajectories and therefore, the cost functional (1) becomes:

$$J = \int_{t_0^{(1)}}^{t_f^{(N)}} FF(t)\,\mathrm{d}t, \quad (16)$$

while dynamic equations (2) are particularised by the point-mass model given by (7).

Event constraints (3) for the state variables fix the initial and final conditions of the problem. In this paper, the initial and final points are taken, respectively, at the moment the slats are retracted (after the take-off) and extended (before the landing). The remaining parts of the take-off and approach are not optimised because almost no degrees of freedom are left for optimisation, since the trajectory is heavily constrained with operational procedures.

The whole state vector is fixed at the final point of the optimisation ($\boldsymbol{x}(t_f^{(N)})$) with the values of the state variables obtained with the initial guess trajectory at this point (see section IV-C). For the initial point of the optimisation ($\boldsymbol{x}(t_0^{(1)})$), however, the mass of the aircraft is not fixed (it will be determined be the optimisation itself, since the trip fuel is being minimised) being all the remaining state variables fixed to the corresponding values of the initial guess trajectory at this initial point (slats retraction).

Generic box constraints on the state and control variables (5) are specified as follows:

$$\gamma_{min} \leqslant \gamma \leqslant \gamma_{max}\,; \quad 0 \leqslant \pi \leqslant 1; \quad (17)$$

where γ_{min} and γ_{max} are aircraft dependent scalars. Note that there is no need to bound the state variable v, since it will be bounded implicitly by the following path constraints set for v_{CAS} and M:

$$M \leqslant MMO\,; \quad v_{CAS} \leqslant VMO; \quad (18)$$

where MMO and VMO are, respectively, the maximum operational Mach and calibrated speed.

Link constraints (6) are defined at each phase boundary imposing continuity to all state variables:

$$\boldsymbol{x}^{(i)}(t_f^{(i)}) = \boldsymbol{x}^{(i+1)}(t_0^{(i+1)})\,; \quad i = 1, \ldots, N-1 \quad (19)$$

Current (or conventional) operations are subject to several operational constraints. In this paper, these operations are compared with an hypothetical unconstrained flight (or *perfect* flight). Next, the different constraints modelled in the two proposed scenarios are specified.

A. Constraints for conventional operations

The most important constraint of current ConOps is perhaps the requirement to fly at a constant cruise altitude. In general, the lower the aircraft mass the higher the most fuel-efficient cruise altitude. Thus, since aircraft is continuously burning fuel (and thus, losing weight) operators can plan in advance one or more step-climbs for long-haul flights. These changes of altitude are always subject to ATC approval and are typically performed with 2000 ft intervals. Minimum distances and/or times are typically enforced to avoid too short cruises.

According to FAA and EASA regulations, a minimum rate of climb of $ROC_{min} = 500$ ft/min is enforced to all aircraft in order to ensure that controllers can predict flight profiles to maintain standard separation. Moreover, in some controlled airspaces aircraft should not operate with a climb or descent rate exceeding 8000 ft/min [20]. These constraints are enforced in the whole trajectory, being minimum ROC especially relevant for the climbs between two cruise altitudes, since it can limit the capability to climb to a higher cruise altitude. Moreover, ATC procedures typically restrict the calibrated speed of aircraft under FL100 to 250 kt [21].

All previous requirements are modelled in terms of additional path constraints (4) and are in general phase dependent.

For the cruise phases (at constant Mach and altitude), climb phases in between are modelled to enable step climbs as fuel is burned. Path constraints are specified in such a way that the optimiser can freely chose the number of steps climbs to perform. Before reaching the top of descent (TOD), a deceleration cruise phase (at constant altitude) is introduced allowing the aircraft to reach the optimal descent Mach.

Constant Mach, CAS or altitude phases are imposed by means of optimisation parameters that are bounded with upper and lower values. Let $p_M^{(i)}$, $p_{v_{CAS}}^{(i)}$ and $p_h^{(i)}$ be these new optimisation parameters at phase i and respectively for M, v_{CAS} and h constraints. It should be noted that $p_{v_{CAS}}^{(i)}$ and $p_M^{(i)}$ can take any continuous value between the upper and lower bounds. On the other hand, in order to comply with ATC rules, p_h^i is restricted to take discrete values given by flight levels.

Table I wraps-up, for each phase, the different path constraints needed to model current conventional operations. It should be noted that for the sake of simplicity, the phase dependency has been dropped from the notation in this table, except for those cases where confusion could be possible. Thus, equations appearing at each row of this table should be considered only for the concerned phase.

B. Constraints for continuous operations

For continuous operations, the trajectory has been modelled with just one phase in absence of additional constraints. Therefore, only event constraints in order to fix the initial and final conditions of the problem along with generic box (17) and path (18) constraints have been considered.

TABLE I
PATH, BOX AND EVENT CONSTRAINTS FOR EACH PHASE OF THE CONVENTIONAL OPERATIONS TRAJECTORY MODEL

Phase	Description	Path Constraints	Event or Box Constraints
1	Initial acceleration	$\dot{v}_{CAS}(t) \geqslant 0$	
2	Constant CAS climb	$v_{CAS}(t) = p_{CAS}^{(2)}\ ;\ p_{CAS}^{(2)} \leqslant 250$ kt	
3	Climb acceleration	$\dot{v}_{CAS}(t) \geqslant 0$	$h(t_0) = 10000$ ft
4	Constant CAS climb	$v_{CAS}(t) = p_{CAS}^{(4)}\ ;\ p_{CAS}^{(4)} \leqslant VMO$	
5	Constant Mach climb	$M(t) = p_M^{(5)}\ ;\ p_M^{(5)} \leqslant MMO$	
6	Cruise	$M(t) = p_M^{(6)}\ ;\ p_M^{(6)} \leqslant MMO$ $h(t) = (2p_h^{(6)} + 1)1000$ ft $;\ 14 \leqslant p_h^{(6)} \leqslant 21$	$t_f \geqslant t_0 + \Delta t_{min}^{(cruise)}$ $s(t_f) \geqslant s(t_0) + \Delta s_{min}^{(cruise)}$
7	Step climb	$M(t) = p_M^{(7)}\ ;\ p_M^{(7)} \leqslant MMO$	$t_f \leqslant t_0 + \frac{h^{(8)} - h^{(6)}}{ROC_{min}}$
8	Cruise	$M(t) = p_M^{(8)}\ ;\ p_M^{(8)} \leqslant MMO$ $h(t) = (2p_h^{(8)} + 1)1000$ ft $;\ 14 \leqslant p_h^{(8)} \leqslant 21$	$t_f \geqslant t_0 + \Delta t_{min}^{(cruise)} \left(p_h^{(8)} - p_h^{(6)}\right)$ $s(t_f) \geqslant s(t_0) + \Delta s_{min}^{(cruise)} \left(p_h^{(8)} - p_h^{(6)}\right)$
...	...	...	...
k	Step climb	$M(t) = p_M^{(k)}\ ;\ p_M^{(k)} \leqslant MMO$	$t_f \leqslant t_0 + \frac{h^{(k+1)} - h^{(k-1)}}{ROC_{min}}$
$k+1$	Cruise	$M(t) = p_M^{(k+1)}\ ;\ p_M^{(k+1)} \leqslant MMO$ $h(t) = (2p_h^{(k+1)} + 1)1000$ ft $;\ 14 \leqslant p_h^{(k+1)} \leqslant 21$	$t_f \geqslant t_0 + \Delta t_{min}^{(cruise)} \left(p_h^{(k+1)} - p_h^{(k-1)}\right)$ $s(t_f) \geqslant s(t_0) + \Delta s_{min}^{(cruise)} \left(p_h^{(k+1)} - p_h^{(k-1)}\right)$
...	...	...	...
$N-6$	Cruise	$h(t) = (2p_h^{(N-6)} + 1)1000$ ft $;\ 14 \leqslant p_h^{(N-6)} \leqslant 21$	$t_f \geqslant t_0 + \Delta t_{min}^{(cruise)} \left(p_h^{(N-6)} - p_h^{(N-8)}\right) - \Delta t^{(N-5)}$ $s(t_f) \geqslant s(t_0) + \Delta s_{min}^{(cruise)} \left(p_h^{(N-6)} - p_h^{(N-8)}\right) - \Delta s^{(N-5)}$
$N-5$	Cruise deceleration	$h(t) = (2p_h^{(N-5)} + 1)1000$ ft $;\ 14 \leqslant p_h^{(N-5)} \leqslant 21$	
$N-4$	Constant Mach descent	$M(t) = p_M^{(N-4)}\ ;\ p_M^{(N-4)} \leqslant MMO$	
$N-3$	Constant CAS descent	$v_{CAS}(t) = p_{CAS}^{(N-3)}\ ;\ p_{CAS}^{(N-3)} \leqslant VMO$	
$N-2$	Descent deceleration	$\dot{v}_{CAS}(t) \leqslant 0$	
$N-1$	Constant CAS descent	$v_{CAS}(t) = p_{CAS}^{(N-1)}\ ;\ p_{CAS}^{(N-1)} \leqslant 250$ kt	$h(t_0) = 10000$ ft
N	Final deceleration	$\dot{v}_{CAS}(t) \leqslant 0$	

NOTE: For this paper we have considered $\Delta t_{min}^{(cruise)} = 5$ min and $\Delta s_{min}^{(cruise)} = 50$ NM for all conventional trajectories.

C. Generation of the initial guess trajectory

The initial guess trajectory generated in this study for both conventional and continuous operations consists of an uninterrupted continuous climb followed by a single cruise at a constant altitude and a continuous descent towards the destination airport. Each segment is divided in several phases with different models and standard operational procedures (such as constant CAS or constant Mach climbs and descents). Then an initial value problem is set for each phase and the trajectory is found by numerical integration of (7).

Since the take-off mass at the origin airport is unknown (depends on the trip fuel, which is unknown) a backwards integration of (7) is initially done up to a given cruise altitude, starting at the runway threshold and assuming a thrust-idle descent. Then an estimation of the take-off mass is done, based on historical data from previous simulations and a forward integration is done from the departing runway threshold up to the TOD. An iterative process is implemented in order to refine at each step the initial mass estimation up to the point the mass discrepancy at the TOD with previous backwards integration is below a user defined tolerance.

Another iterative process is also implemented in order to determine the best cruise altitude. This results with a very accurate (and feasible) trajectory that helps significantly the convergence and reduces the execution time of the optimisation algorithm.

V. NUMERICAL RESULTS

This section compares the results (in terms of fuel consumption and flight time) between conventional and continuous operations for several case studies using an Airbus A320, a typical twin-engine, narrow-body, transport aircraft.

A. Experimental setup

A set of representative A320 trip distances between 400 NM and 2400 NM have been chosen for this study. For each trip distance, the optimal conventional and continuous operations trajectories from slats retraction to flaps extension have been computed for several landing masses between the operative empty mass and maximum landing mass (MLM). Results were obtained using solvers CONOPT (as NLP) and SBB as MINLP (mixed integer nonlinear programming), both bundled into the GAMS software suite. Finally, in this study and regarding conventional operations, odd flight levels have been considered

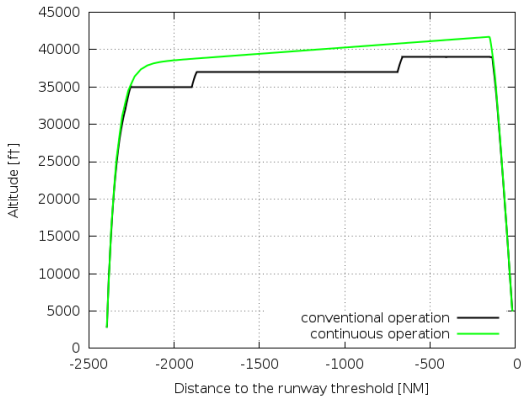

(a) Optimal trajectories for 87% of maximum landing mass

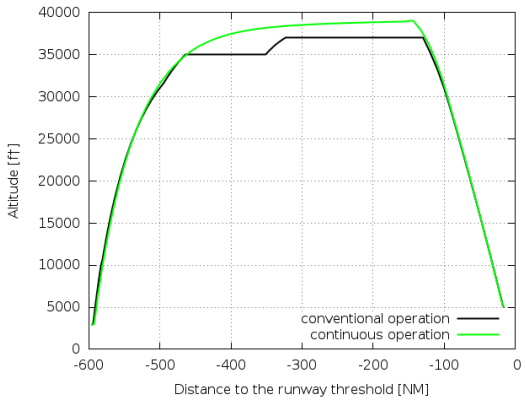

(b) Optimal trajectories for 99% of maximum landing mass

Fig. 1. Examples of optimal trajectories

allowing the algorithm to perform a maximum number of three possible step climbs. Fig. 1 shows two examples of optimal trajectories computed with previous algorithms.

These results are consistent with those found in the literature [3], [5], [22], where unconstrained trajectories follow the so called a *cruise climb*, i.e. a continuous climb up to the TOD, where the continuous descent is initiated. For aircraft equipped with jet engines, the higher the altitude the more fuel-efficient the engine becomes and therefore, the aircraft seeks to achieve the maximum altitude in the minimum amount of time. An optimal altitude is found where fuel consumption is minimised by flying at the most efficient speed and engine setting. As fuel is burned and aircraft weight decreases, the amount of lift needed and, consequently, the drag are reduced meaning that the required thrust is also lower. If throttle is reduced then the engine is not longer operating at the most efficient setting. Therefore, the optimal procedure is to maintain the most efficient speed and power setting and using the excess thrust to slowly climb the aircraft. Cruise climb ends when the optimum descent path is intercepted. This path is the result of descending continuously at minimum gradient (or minimum drag) speed, which allows the aircraft to maximise the flown distance at idle thrust.

Conventional procedures shown in Fig. 1 are also consistent with optimal constrained flight profiles [3], [12], where step climbs are performed at the moment this excess thrust allows the aircraft to climb at the minimum rate of climb required by operational constraints. Due to this restriction, conventional vertical profiles are always below continuous climb profiles: for a given mass, increasing the altitude decreases the specific excess power and therefore, the rate of climb performance. Thus a maximum altitude will be found, such as the aircraft can reach it with the minimum allowed rate of climb. Then, as fuel is burned while cruising at this constant altitude the rate of climb available increases up to the point a step climb can be performed up to the next available cruise altitude.

B. Results

Fig. 2 shows the optimal trip fuel for both conventional and continuous operations, as a function of the considered distances and landing masses. As expected, the amount of fuel needed increases with the total trip distance and landing mass. Moreover, for a same case continuous operations require less fuel if compared with the conventional scenario. Fig. 3 shows these fuel savings in absolute and relative terms. These results agree with those obtained in the AIRE flight trials [23], where potential savings around 300 kg of fuel where observed on the route Keflavik-Seattle (6680 NM). As seen from Fig. 3(b), large relative savings are also observed for long-haul flights. In this case, however, is much harder to establish a correlation between the relative savings and the landing mass of the aircraft.

The discontinuities observed in the previous plots are mainly due to the discrete behavior of the conventional operations. For example, as long as the landing mass decreases progressively, the optimal altitude increases progressively too. Yet, since only discrete cruise altitudes are allowed, this optimal flight altitude will suddenly change at some landing mass, producing a discontinuity to the fuel consumption.

It should be noted that in our analysis the conventional flight is somehow idealised since climb and descent paths have relaxed constraints allowing continuous climbs and descents. Nowadays, these continuous operations are not usually performed as level-offs and/or path stretching are mandated by ATC in order to maintain separation, especially in busy terminal airspaces. Moreover, in some controlled airspaces the ATC may also bound upper and/or lower airspeeds in order to facilitate the traffic flow separation and the ATC tasks. These speed restrictions may also induce some extra fuel consumption, since climbs and/or descents cannot be longer flown at the optimal speeds.

Ref. [8], for instance, studies the effect of level segments in descent procedures, showing average fuel savings of approximately 200 kg flight. Another quantitative example is given in [24], where some flights trials from Edinburg to London were performed flying an uninterrupted climb to cruise altitude followed by a direct route (at constant altitude) and an uninterrupted descent. For these trials, fuel reduction was found to be around the 10% of the total trip fuel (also around 300 kg). Thus, the observed fuel savings in our study are

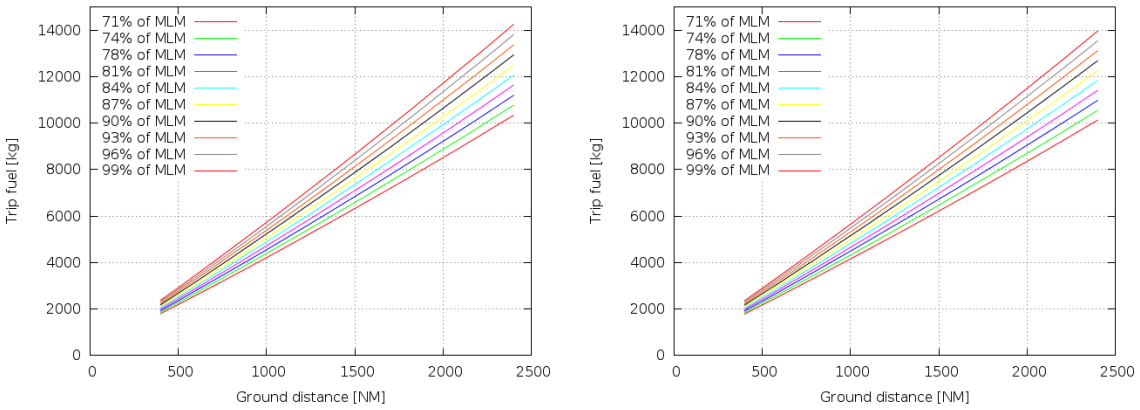

(a) Conventional operations

(b) Continuous operations

Fig. 2. Total trip fuel obtained after the optimisation process as a function of trip distance and landing mass

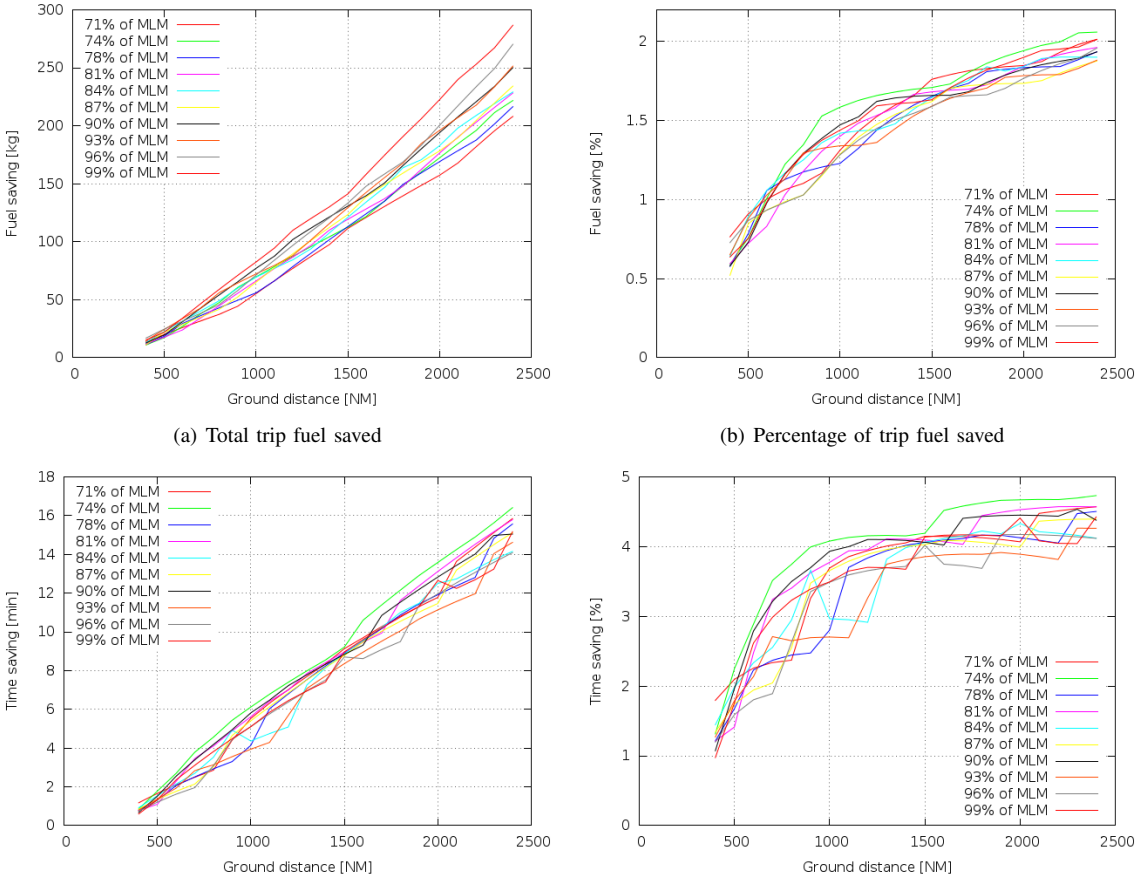

(a) Total trip fuel saved

(b) Percentage of trip fuel saved

(c) Total trip time saved

(d) Percentage of trip time saved

Fig. 3. Trip fuel and trip time savings by flying continuous operations with respect to conventional operations

mainly achieved by the possibility to fly a continuous cruise climb and should be added to these potential savings due to continuous climb/descent operations and direct routings.

In this study, trip time differences have also been analysed. Fig. 3 presents these differences in absolute and relative terms. It is very interesting to note that continuous operations not only represent lower fuel consumptions but also shorter trip times.

As shown in [2], for a given mass the Mach that minimses fuel consumption increases with altitude and an optimal altitude can also be found (with its corresponding optimal Mach). Yet, this altitude cannot always be reached due to engine performance limitations. In continuous operations, the aircraft is following this optimal altitude (that increases as long as the mass of the aircraft decreases). For conventional

operations, however, the aircraft must cruise at a lower altitude in order to have the required excess thrust needed to fulfill the minimum rate of climb constraint. Thus, the aircraft flies at a less fuel-efficient altitude, which leads to a lower cruise speed (if compared with the higher speed that it would have at the optimal altitude). Consequently, this difference in cruise altitude produces more fuel consumption and more trip time.

VI. Conclusion

The reduction of fuel consumption (and gaseous emissions) is one of the major drivers of current research efforts in air transportation. Even small amounts of fuel savings become significant at aggregate level, especially when we consider the high volume of traffic that is operating every day. This paper has focused on the potential savings of the introduction of eventual continuous cruise climb operations for an Airbus A320, showing already some remarkable figures in terms of fuel consumption, mainly for longer routes.

Another important remark that arises from this study is that continuous operations not only reduce fuel consumption, but also the trip time. This is particularly interesting since aircraft operators typically seek to optimise a trade-off between fuel and time consumption for a given flight. Thus, the economic benefit of such continuous operations is twofold.

In this paper, conventional operations have been computed considering a maximum range scenario (i.e. the operator aims at minimising the total trip fuel). Current operations, however, are performed at higher cruise speeds (thus, incurring extra fuel consumption), since the cost of the time is also considered for flight planning. Therefore, fuel savings of continuous cruise climb operations would be even larger if compared with these cost-based operations.

Future work will study long-haul aircraft (such as the A330 or A340), since fuel and time savings are expected to be more relevant. Moreover, a sensibility study on the influence of real weather scenarios (and in particular wind fields) on fuel consumption figures is also foreseen. Also a scenario based investigation with a variation of the relevant parameters (e.g. realistic climb/descent rates) would have been interesting and should be focused in future work.

According to SESAR and NextGen paradigms, new avionic systems will be able to support trajectory-based operations in the forthcoming years. In a futuristic scenario, we could envisage that aircraft themselves are responsible for keeping separation amongst each other, thus delegating air traffic control responsibilities to the pilot by means of airborne separation assurance systems (ASAS) [25]. Fuel and time savings shown in this paper can endorse and motivate future research efforts in separation assurance to make such continuous cruise climb operations safe and operationally sound.

Acknowledgment

The authors would like to thank Airbus Industrie for the use of PEP (Performance Engineers Program) suite, which allowed us to undertake realistic aircraft performances simulations.

References

[1] IATA, "IATA economic briefing. Airline fuel and labour cost share," 2010.

[2] E. L. Miller, "Optimal cruise performance," *Journal of Aircraft*, vol. 30, no. 3, pp. 403–405, May 1993.

[3] M. Soler, A. Olivares, E. Staffetti, and D. Zapata, "Framework for aircraft trajectory planning toward an efficient air traffic management," *Journal of Aircraft*, vol. 49, no. 1, pp. 341–348, Jan. 2012.

[4] R. H. Veenstra, "Commercial aircraft trajectory optimization and efficiency of air traffic control procedures," Master's thesis, University of Minnesota, Nov. 2011.

[5] J. A. Lovegren and R. J. Hansman, "Estimation of potential aircraft fuel burn reduction in cruise via speed and altitude optimization strategies," MIT International Center for Air Transport (ICAT), Cambridge, USA, Tech. Rep., Feb. 2011.

[6] J. A. Sorensen and M. H. Waters, "Generation of optimum vertical profiles for and advanced flight management system," NASA, Mountain View, California, Tech. Rep. 165674, march 1981.

[7] H. Erzberger, J. D. Mclean, and J. F. Barman, "Fixed-range optimum trajectories for short-haul aircraft," NASA, Washington, D.C., Tech. Rep. D-8115, Dec. 1975.

[8] T. Thompson, B. Miller, C. Murphy, S. Augustine, T. White, and S. Souihi, "Environmental impacts of continuous-descent operations in Paris and New York regions. Isolation of ATM/airspace effects and comparison of models," in *Proceedings of the Tenth USA/Europe Air Traffic Management Research and Development Seminar (ATM2013)*, Chicago, Illinois (USA), Jun. 2013.

[9] J. B. Clarke, N. T. Ho, L. Ren, J. A. Brown, K. R. Elmer, K. Zou, C. Hunting, D. L. McGregor, B. N. Shivashankara, K. Tong, A. W. Warren, and J. K. Wat, "Continuous descent approach: Design and flight test for Louisville international airport," *Journal of Aircraft*, vol. 41, no. 5, pp. 1054–1066, Sep. 2004.

[10] L. Jin, Y. Cao, and D. Sun, "Investigation of potential fuel savings due to continuous-descent approach," *Journal of Aircraft*, vol. 50, no. 3, pp. 807–816, Feb. 2013.

[11] A. Valenzuela, "Aircraft trajectory optimization using parametric optimization theory," Ph.D. dissertation, Univeristy of Seville, Nov. 2012.

[12] J. T. Betts and E. J. Cramer, "Application of direct transcription to commercial aircraft trajectory optimization," *Journal of Guidance, Control, and Dynamics*, vol. 18, no. 1, pp. 151–159, Jan. 1995.

[13] M. Kaiser, M. Schultz, and H. Fricke, "Enhanced jet performance model for high precision 4D flight path prediction," in *Proceedings of the 1st International Conference on Application and Theory of Automation in Command and Control Systems (ATACCS)*, 2011, pp. 33–40.

[14] J. T. Betts, *Practical methods for optimal control using nonlinear programming*, ser. Advances in Design and Control. Philadelphia, U.E: Society for Industrial and Applied Mathematics (SIAM), 2001, vol. 3.

[15] ——, "Survey of numerical methods for trajectory optimization," *Journal of Guidance, Control, and Dynamics*, vol. 21, no. 2, pp. 193–207, Mar. 1998.

[16] GAMS, *GAMS: The Solver Manuals*, GAMS Development Corporation, Nov. 2013.

[17] D. G. Hull, *Fundamentals of airplane flight mechanics*, 1st ed. Springer Publishing Company, Incorporated, 2007.

[18] ICAO, "Manual of the ICAO Standard Atmosphere: Extended to 80 Kilometres (262500 Feet)," International Civil Aviation Organization, Montreal, Canada, Tech. Rep., 1993.

[19] Air Force Test Pilot School, Edwards AFB, CA, "Cruise performance theory," in *Performance phase*, Sep. 1993, vol. 1, ch. 11.

[20] G. B. C. A. Authority, "Aeronautical information publication (AIP) United Kingdom: En-route (ENR) 1.1 - general rules," 2013.

[21] F. A. A. U.S. Dept. of Transportation, "Aeronautical information publication (AIP): Subchapter F - Part 91," pp. 579–844, Jan. 2012.

[22] J. García-Heras, F. J. Sez-Nieto, and R. Román, "Aircraft trajectory simulator using a three degrees of freedom aircraft point mass model," in *Proceedings of the 3rd International Conference on Application and Theory of Automation in Command and Control Systems (ATACCS)*, 2013, pp. 114–117.

[23] SESAR Joint Undertaking, "AIRE project results 2009," 2010.

[24] NATS, "NATS Fuel Efficiency Metric," Jan. 2012.

[25] Eurocontrol, "Review of ASAS applications studied in europe," CARE/ASAS Action – Activity 4, Technical report, Feb 2002.